

See discussions, stats, and author profiles for this publication at: <https://www.researchgate.net/publication/283618705>

Combined Effect of Pyrolysis Pressure and Temperature on the Yield and CO₂ Gasification Reactivity of Acacia Wood in macro-TG

Article in *Energy & Fuels* · October 2015

DOI: 10.1021/acs.energyfuels.5b01454

CITATIONS

33

READS

790

4 authors, including:



Eric Serges Noumi

Research & Innovation Centre for Energy (RICE)

9 PUBLICATIONS 209 CITATIONS

[SEE PROFILE](#)



Joel Blin

Cirad - La recherche agronomique pour le développement

113 PUBLICATIONS 4,036 CITATIONS

[SEE PROFILE](#)



Patrick Rousset

Cirad - La recherche agronomique pour le développement / JGSEE / KMUTT / KU

74 PUBLICATIONS 2,328 CITATIONS

[SEE PROFILE](#)

Combined Effect of Pyrolysis Pressure and Temperature on the Yield and CO₂ Gasification Reactivity of Acacia Wood in macro-TG

Eric S. Noumi,^{†,§} Joel Blin,^{*,†,‡} Jeremy Valette,[‡] and Patrick Rousset^{‡,§,⊥}

[†]International Institute for Water and Environmental Engineering (2iE), Ouagadougou Campus, Rue de la Science, 01 BP 594 Ouagadougou, Burkina Faso

[‡]French Agriculture Research Centre for International Development (CIRAD), 73 Rue J. F. Breton, 34398 Cedex 5 Montpellier, France

[§]University of Brasilia, Brasilia, Distrito Federal CEP 70910-900, Brazil

ABSTRACT: This work examines the effect of both absolute pressure (range 1–6 bar) and peak temperature (range 350–800 °C) during pyrolysis of acacia wood in a macro-TG on the yield and CO₂ gasification reactivity of the resulting charcoal. A central composite design was used for the experiments. The results of statistical analyses showed satisfactory agreement between the experimental results (charcoal yield and charcoal CO₂ gasification reactivity) and model predictions. Both charcoal yield and reactivity decreased with an increase in temperature but increased with an increase in pressure. An increase in pyrolysis pressure increased charcoal yield and decreased reactivity. The temperature had a more significant effect on charcoal reactivity than pressure, and their interaction was not significant. The optimal conditions for the preparation of reductant charcoal were found to be a peak pyrolysis temperature of 617 °C and an absolute pressure of 6 bar.

1. INTRODUCTION

In recent years, an increasing number of studies have highlighted the advantages of using charcoal instead of coke in blast furnaces to mitigate global warming.^{1–11} Charcoal is a carbon-rich, porous substance that is produced by thermal decomposition of biomass under oxygen limited conditions and at moderate temperature (<700 °C).^{12,13} Due to its low ash content and lack of sulfur, charcoal is considered to be an ideal reducing agent¹⁴ and is the most promising alternative to coke.^{10,11} Although many indices have been established to assess the quality of coking coals, there is an absence of similar standards for metallurgical charcoal. The main problems encountered when using charcoal instead of coke are linked to charcoal's low compressive strength and the high reactivity. Charcoal with high mechanical strength is required to withstand abrasion, thermal shock, and the weakening reaction with carbon dioxide that occurs in a blast furnace.¹⁵ Carbon monoxide is the *reducing* agent formed by the Boudouard reaction, i.e., the gasification of carbonaceous reductant by carbon dioxide. If the carbonaceous reductant is too reactive, carbon monoxide is produced too quickly, decreasing the residence times of this reducing agent inside the blast furnace, and as a result, the reduction of iron ore is not efficient. The less reactive the charcoal, the greater the advantage of replacing coke with charcoal, especially since the rate of degradation of charcoal inside the furnace influences its friability and the generation of fines. There is no known value of reactivity for a good reductant, as the method applied to measure the reactivity of charcoal does not work for coke since it is impossible to gasify coke in ATG at 900 °C. The majority of studies on optimizing the preparation of the charcoal as a reductant for blast furnaces focused on increasing charcoal yield and fixed carbon content and bulk density.^{12,16–18} Studies that include

the reactivity of charcoal in the determination of optimal pyrolysis conditions are thus needed.

The conventional pyrolysis process is the most widely used method of producing charcoal from biomass. The influence of moisture, peak temperature, vapor residence time, and pressure, which all play a key role in pyrolysis, is well-known. According to the results obtained by Rousset et al.,¹⁸ dry wood is preferable for the production of reductant charcoal because the moisture in wood has a negative effect on the fixed carbon yield and on the bulk density of the resulting charcoal. Peak temperature is the highest temperature reached during pyrolysis aimed at converting biomass into charcoal.¹⁹ During pyrolysis, there is usually a decrease in charcoal yield with an increase in temperature, but an increase in the fixed carbon content. Moderate pressure (up to 10 bar) during biomass pyrolysis appears to increase charcoal yield due to the longer residence time of volatile matter in solid particles.^{18,20,21} Moreover the CO₂ gasification reactivity of charcoal gradually decreases with an increase in temperature.¹⁷ Okumura et al.²² found that CO₂ gasification rates in char generated at 1 bar exhibited approximately twice the gasification reactivity of that obtained at 30 bar. This is because the uniformity of the carbonaceous structure increases with pyrolysis pressure. In that study, the uniformity of carbonaceous structures affected CO₂ gasification reactivity, and decreasing uniformity increased the formation of cavities on the surface of the char during the CO₂ gasification process. This result suggests that, with a high temperature and high pressure, pyrolysis will enable production of less reactive charcoal. But a high pyrolysis temperature also reduces charcoal yield and produces charcoal whose mechanical properties are

Received: June 29, 2015

Revised: October 7, 2015



Table 1. Results of Proximate and Elemental Analyses of *Acacia senegal* Wood

proximate	anal std	% by weight	ultimate	anal std	% by weight
volatile	ISO-5623-1974	66.41	carbon	XP CEN/TS 15104	47.80
ash	ISO-1171-1976	2.11	hydrogen		6.05
fixed carbon	ISO-5623-1974	23.82	nitrogen		0.22
moisture content	ISO-5623-1974	7.67	sulfur		0.14
			oxygen ^a	by difference	43.68

^aKnowing that ash content was 2.11%, the oxygen content was obtained by subtraction.

more vulnerable.²³ Hence, the challenge is to find the best compromise among the pyrolysis parameters to ensure the desired properties are achieved.

As no study has yet been conducted on the combined effect of temperature and pressure on the CO₂ gasification reactivity of charcoal, the overall aim of the study is to investigate how these two parameters and their interaction affect charcoal yields and charcoal CO₂ gasification reactivity.

The precise objective of the present study was to statistically analyze the combined effect of pressure (1–6 bar) and temperature (350–800 °C) on charcoal yield and CO₂ reactivity during gasification of charcoal. The experiments were performed using centimeter scale wood particles in a “macro-TG” reactor.

2. EXPERIMENTAL SECTION

2.1. Materials. The biomass used in this study was *Acacia senegal* (*A. senegal*) wood, which was harvested around the city of Ouagadougou in Burkina Faso. This hardwood has a high density (728 kg/m³).²⁴ To ensure homogeneity of the raw material throughout the course of our study, all of the wood was harvested at the same time, stripped of its bark, and sorted to remove any samples containing defects (knots, slot curvature, and grooves, etc.). The wood was cut into cubes (10 mm × 10 mm × 10 mm). The samples were dried in an oven at 105 °C for 8 h according to the NF EN 14774 procedure and then stored in a desiccator until required for the experiments. Table 1 lists the characteristics of *A. senegal* wood revealed by proximate and ultimate analyses.

The macromolecular composition (lignin, extractives, and holocellulose content) of the sample was determined at the Laboratory of Forest Products (LFP) of the Brazilian Forest Council. Extractive content was determined according to TAPPI 204 om-88, using the total extractive method but using ethanol/toluene instead of ethanol/benzene. Lignin content was obtained by adding soluble and insoluble lignin. Insoluble lignin was determined using the Klason method and soluble lignin using spectrophotometry. Holocellulose content was determined by difference, based on extractive-free wood. The results of macromolecular analysis showed 56.16% holocellulose, 34.48% lignin, and 6.89% extractible. Similar values have been reported for hardwood.^{16,25,26} The high lignin content was also within the ranges reported for hardwood.

2.2. Description of the Experiments. Figure 1 shows the experimental setup with the macro-TG reactor used for the experiments. The equipment is described in detail in Daouk et al.²⁷ Briefly, it consisted of a microbalance (Rubotherm), a steel reactor, a furnace, and a thermocouple. The diameter of the reactor was 25 mm. This device allowed a maximum heating rate of 20 °C/min up to 1,000 °C. Changes in temperature in the reactor were monitored by a thermocouple placed inside the reactor. An online scale made it possible to record instantaneous mass loss (with an accuracy of 0.1 mg). The reaction atmosphere inside the oven was controlled by two bottles, one of N₂ and one of CO₂, connected to the reactor through two Brook 5850S Smart mass flow controllers calibrated for N₂ and CO₂ in a range of 0–400 N mL/min. A Brook 5866 valve calibrated for the 0–50 bar range made it possible to set and maintain the pressure inside the reactor. During testing, the sample was placed in a braided wire basket made of nickel so that all of the surfaces of the

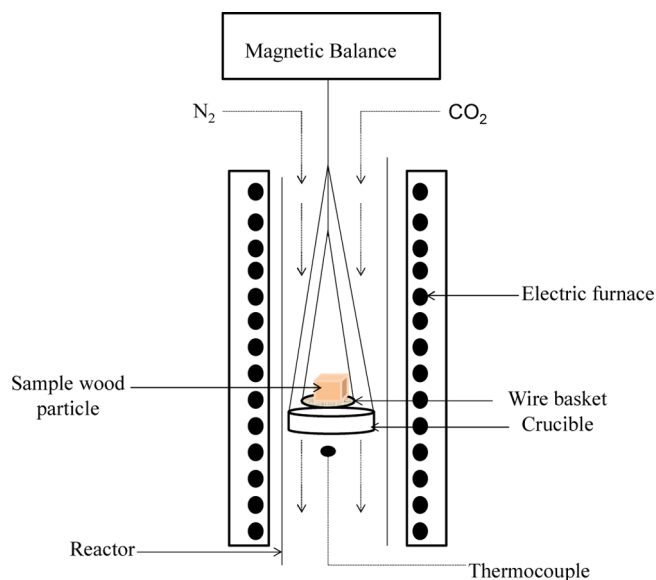


Figure 1. Schematic diagram of the experimental pyrolysis setup.

sample were exposed to a uniform heat flow. To limit systematic errors, the calibration of the electronic balance was checked before each experiment began.

The experiment took place in four steps to allow simultaneous monitoring of charcoal production and CO₂ gasification of the resulting charcoal (Figure 2):

- (i) Drying step:** This was done for 15 min at 120 °C.
- (ii) Pyrolysis stage:** Under the desired N₂ pressure, temperature was increased by 10 °C/min to the peak temperature. The peak temperature was kept constant for 60 min to ensure a stable final mass.
- (iii) Postpyrolysis stage:** After pyrolysis, the pressure was manually reduced to atmospheric pressure. Thereafter the charcoal sample was heated in a flow of N₂ at a rate of 20 °C/min up to 900 °C for gasification. According to Kumar and Gupta,²⁸ this postpyrolysis step should be as rapid as possible to limit major changes in the structure and morphology of the charcoal. The final temperature was kept constant for 10 min to allow the system to stabilize.
- (iv) Charcoal gasification stage:** Upon reaching thermal equilibration at the final temperature of 900 °C, the isothermal gasification reaction of the char sample was started by injecting carbon dioxide. The charcoal was then allowed to react until its weight loss decreased to nearly zero.

At the end of gasification, the experiment was stopped by switching back to nitrogen.

Mass loss was recorded as a function of time during the course of the experiment, which made it possible to calculate the charcoal yield (Y_{char}) (eq 1) during pyrolysis and its degree of conversion (X) (eq 2) and reactivity at time t (R) (eq 3) during the gasification phase).

$$Y_{\text{char}} = \frac{m_{\text{char}}}{m_b} \quad (1)$$

where m_{char} is the mass of the resulting charcoal and m_b is the dry mass of the wood sample.

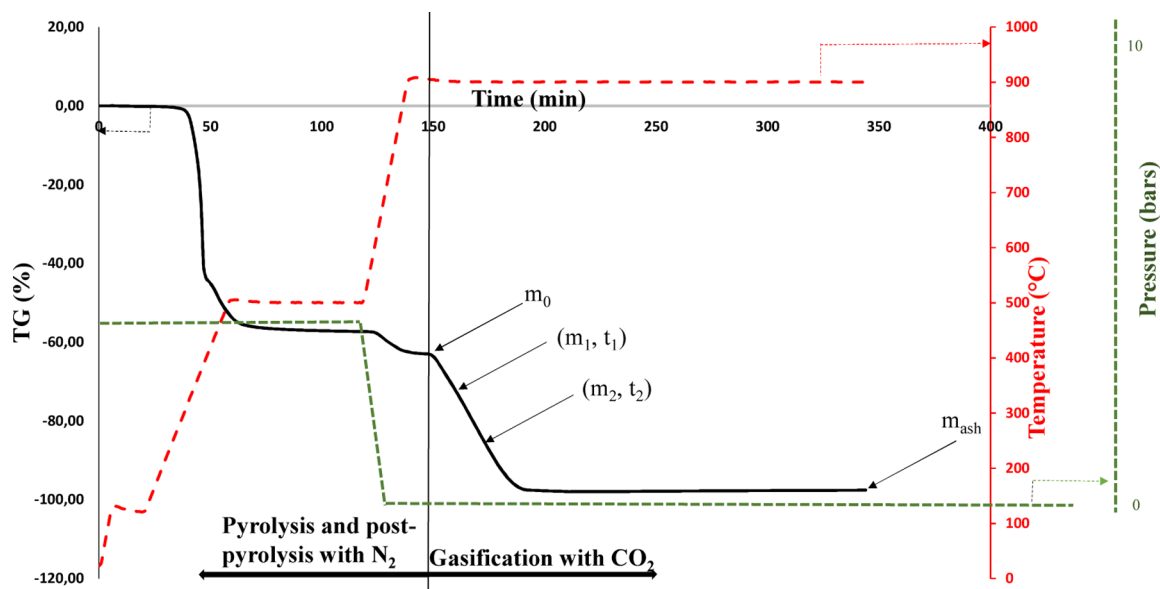


Figure 2. Experimental procedure showing changes in the temperature and in pressure and an example of changes in mass loss by an acacia sample.

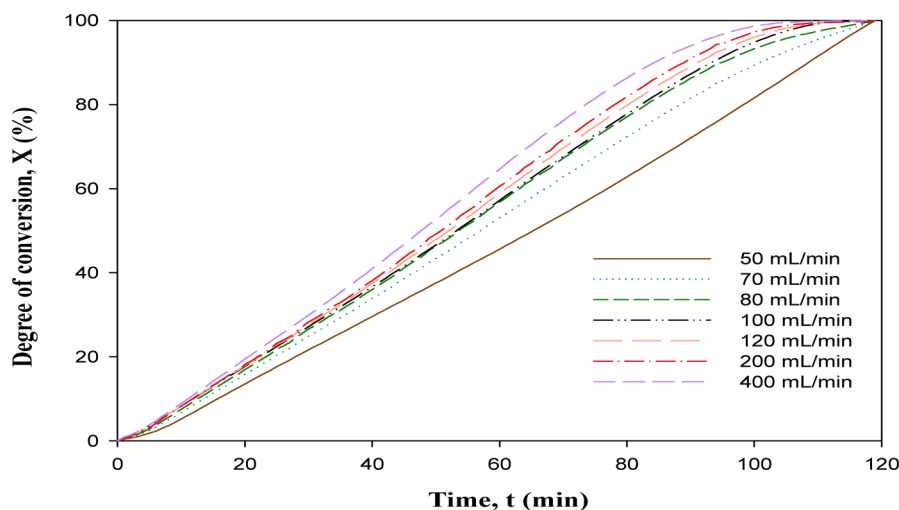


Figure 3. Changes in the char gasification rate in the “macro-TG” reactor as a function of the flow rate of the reactant gas at a temperature of 900 °C.

$$X = \left(1 - \frac{m - m_{\text{ash}}}{m_0 - m_{\text{ash}}} \right) \times 100 \quad (2)$$

$$R = - \frac{dm}{dt} \frac{1}{(m - m_{\text{ash}})} = - \frac{m_2 - m_1}{(t_2 - t_1)(m_1 - m_{\text{ash}})} \quad (3)$$

where m is the instantaneous sample mass during gasification, m_0 is the mass of the sample at the beginning of gasification, m_{ash} is the ash content of the sample, t_1 is the time when the measurement of weight begins, t_2 is the time when the measurement of weight ends, m_1 is the sample mass at t_1 , and m_2 is sample mass at t_2 .

The CO_2 gasification reactivity of charcoal is a continuous function over time (eq 3), and a representative value is required for each experiment. There is no consensus in the literature on how to define a representative value of reactivity for an experiment. The most frequently used value is the average reactivity between two degrees of conversion: for instance, 0–50%,²⁹ 0–95%,³⁰ 60–80%,³¹ and 20–80%.³² This can also correspond to reactivity at a specific conversion: for instance, 50%.^{33,34} The range of conversion chosen depends on the criteria selected by the author. In the present study, we chose the average reactivity between 20% and 80% of conversion as the representative value to obtain the reactivity of the experiment, as

Barrio et al.³² showed that the value of reactivity obtained in this range is more precise.

The gasification of char biomass is affected by external diffusion of the reactant gas. Preliminary macro-TG tests were conducted to eliminate these influences and also to fix the flow rate of the reactant gas. To avoid the influence of external diffusion on the charcoal gasification rate, researchers usually have to determine the range of reactant gas flow for which there is no appreciable difference in the gasification rate curve.^{35,36}

Figure 3 shows the curves obtained when studying the influence of the flow rate of the reactant gas (CO_2) on the char gasification rate in the macro-TG reactor. The degree of conversion increased with an increase in the flow rate of the reactant gas, but with a flow rate ranging from 80 to 120 mL/min, the conversion curves of the charcoal are almost superimposed. So for this work, the flow of N_2 or CO_2 used was 100 mL/min.

2.3. Experimental Design. The response surface methodology (RSM) consists of a group of mathematical and statistical techniques that can be used to define the relationships between the responses and the independent variable.³⁷ RSM has several advantages over standard experimental or optimization methods in which one variable is used at a time: it can provide a large amount of information from a small number of experiments, and, in RSM, it is possible to observe the

effect of the interaction between the independent parameters on the response. In the present study, a two-level face-centered central composite design (FCCCD) was used to statistically analyze the effects of the selected factors, i.e., temperature and pressure. This type of design is appropriate to build a second-order response surface model.³⁸ Second-order models make it possible to account for the nonlinear nature of the response surface, which is impossible using a first-order statistical design. "Statgraphics" software was used to design the experimental matrix and to perform the necessary statistical analyses. The two response variables related to charcoal characteristics analyzed were (i) charcoal yield (Y_{char}) and (ii) charcoal reactivity to CO_2 gasification (R). To fix the range of variation of the dependent variables, peak temperature (T) and absolute pressure (P), the results obtained by Rousset et al.¹⁸ were exploited. These authors performed a statistical analysis of the impact of pressure on the quality of the resulting charcoal using *Eucalyptus grandis* (*E. grandis*) wood.¹⁸ Three relative working pressures (0, 5, and 10 bar), two carbonization temperatures (450 and 600 °C), and three wood moisture contents (0, 15 and 110%) were used. They found that the best "steel" quality charcoal was obtained using a dry wood, a pressure of 10 bar, and a temperature of 600 °C. Based on these results and the technological advances in the design of industrial reactors, in our study, we set the range of the pyrolysis pressure to 1–6 bar and the range of temperature to 350–800 °C (Table 2).

Table 2. Summary of the Experimental Conditions

	Pyrolysis step		Gasification step
	Minimum	Maximum	
Temperature	350 °C	800 °C	
Heating rate	10 °C/min up to the final temperature and 60 min isothermal at final temp.		Isotherm at 900 °C
Pressure	1 bar	6 bars	Atmospheric pressure
Gas flow	N_2 at 100 ml/min		CO_2 at 100 ml/min

To estimate the variance of the experimental error and the overall curvature effect, three replicates were carried out at A temperature of 575 °C and a pressure of 3.5 bar. Through the repeatability of the experiments, the error bars of charcoal yield and reactivity were estimated to be about 0.29% and 5%, respectively. Given the heterogeneity of the wood sample, these values were considered to be acceptable. The experimental sequence of the two-level face-centered central composite design was randomized in order to minimize the effects of the uncontrolled factors. However, it should be noted that the response surface models we obtained are only valid in the ranges of the parameters we selected.

3. RESULTS AND DISCUSSION

In this section, we present and discuss our experimental results for the response variables. We used multivariate analysis to determine the most appropriate pyrolysis conditions for the synthesis of reductant charcoal.

3.1. Response Analysis and Interpretation. Table 3 lists charcoal yields (Y_{char}) and the CO_2 gasification reactivity of the resulting charcoal (R) measured during the experiments. Charcoal yield ranged from 32.39% to 52.40%; the smallest charcoal yields were obtained at a high peak pyrolysis temperature and the biggest yields at a low peak pyrolysis temperature. The average CO_2 gasification reactivity obtained ranged from 14.51×10^{-3} to 22.32×10^{-3} g/(g·min). Maximum reactivity was obtained at a temperature of 350 °C and a pressure of 1 bar and minimum reactivity at a temperature of 800 °C and a pressure of 6 bar.

Each response variable (Y_{char} and R) was analyzed using the response surface method (RSM) to build a regression model reflecting the quantitative influence of factors T and P . Thus, from the experimental data generated using the previously mentioned FCCCD approach, functional relationships between

Table 3. Experimental Results Obtained with the Central Composite Design

run	coded factors		real factors		responses	
	X_1	X_2	temp (°C)	pressure (bars)	Y_{char} (%)	R (10^{-3} g/(g·min))
1	−1	−1	350	1	49.51	22.32
2	0	0	575	3.5	37.69	19.30
3	0	0	575	3.5	37.48	19.32
4	1	−1	800	1	32.39	15.88
5	0	0	575	3.5	37.59	19.37
6	−1	1	350	6	52.40	20.26
7	1	1	800	6	33.85	14.51
8	0	1	575	6	40.87	16.77
9	1	0	800	3.5	33.12	14.59
10	0	−1	575	1	34.76	19.80
11	−1	0	350	3.5	50.62	21.51
12	0	0	575	3.5	38.33	18.57

the response (Y) and the coded independent variables (X_1 for T and X_2 for P) can be quantified using the estimated parameters of a second-order regression model (eq 4).

$$Y = \beta_0 + \beta_1 X_1 + \beta_2 X_2 + \beta_{11} X_1^2 + \beta_{22} X_2^2 + \beta_{12} X_1 X_2 \quad (4)$$

where β_0 is the constant coefficient, β_1 and β_2 are the linear coefficients, β_{11} and β_{22} are the quadratic coefficients, and β_{12} is the interaction coefficient. These coefficients were calculated from the experimental responses by least-squares regression using Statgraphics software. A positive coefficient in the response function indicates positive correlations (i.e., a synergistic effect) between the corresponding independent variable and the response, whereas a negative coefficient indicates an antagonistic effect.

In the following sections, the results of the statistical analysis for each response variable are presented and discussed. The polynomial model equation in terms of coded factors is as follows:

$$Y_{\text{char}} = 37.7517 - 8.861X_1 + 1.743X_2 + 4.160X_1^2 - 0.357X_1X_2 + 0.105X_2^2 \quad (5)$$

$$R = 18.965 - 3.185X_1 - 1.076X_2 - 0.566X_1^2 + 0.172X_1X_2 - 0.331X_2^2 \quad (6)$$

So, for the response Y_{char} , one can see that T has an antagonistic effect and P has a synergistic effect and that, for the response R , both T and P have an antagonistic effect.

The R^2 and the R^2_{adj} values obtained are respectively 0.9897 and 0.9811 for Y_{char} and 0.949 and 0.9495 for R . This means that 98.9% of the total variation in charcoal yield and 94.9% of the total variation in charcoal reactivity can be attributed to the variation in T and P . This also means that there is approximately 1.1% and 5.1% chance that the variations in charcoal yield and charcoal reactivity respectively are due to noise, showing that the prediction values for the responses are accurate (95% confidence limit).

The credibility of the model response was further evaluated by analysis of variance (ANOVA) at the 5% significance level. The lower the significance level, the more the data must diverge from the null hypothesis to be significant. The results of ANOVA of charcoal yield (Y_{char}) are given in Table 4; the

model p -value (0.0001) is less than 0.05, implying the model is significant.

Table 4. Analysis of Variance of Charcoal Yield, Y_{char} (Y_1)^a

source of variation	sum of squares	degrees of freedom	mean square	F-value	p-value prob > F
model	542.74	5	108.55	115.36	<0.0001***
lack of fit	5.21	3	1.74	11.93	0.0356**

^aEffects: ***, most significant; **, less significant.

Similarly, the effects of the linear, interaction, and quadratic coefficients on charcoal yield based on ANOVA are listed in Table 5. As can be seen, the linear terms of T and P , and the

Table 5. Statistical Estimations of Coefficients for Charcoal Yield, Y_{char} ^a

name	coefficient	F-inflation	std dev	F-value	p-value
β_1	-8.861	1.0	0.311439	3238.50	0.0000***
β_2	1.743	1.0	0.311439	125.34	0.0015**
β_{12}	-0.357	1.125	0.381434	3.51	0.1575*
β_{11}	4.160	1.0	0.467159	317.19	0.0004**
β_{22}	0.105	1.125	0.467159	0.20	0.6835*

^aEffects: ***, most significant effect; **, less significant effect; * effect not significant (5% probability).

quadratic term of T , are significant model parameters (their corresponding p -value is less than 0.05). Manyà et al.³⁹ and Rousset et al.¹⁸ obtained similar results with significant effects of temperature and pressure. The interaction between T and P , and the quadratic term of P , was more significant (their corresponding p -value was >0.05). Unlike our study, Rousset et al. showed that the interaction term of PT ($\beta_{12} = -0.357$ in our case) had a significant effect. In addition, we found that the contribution of significant terms to charcoal yield was in the order ($\beta_1 = -8.861$) > ($\beta_{11} = 4.160$) > ($\beta_2 = 1.743$); i.e., the effect of $T > TT > P$.

Figure 4 shows the two- and three-dimensional surface responses constructed to show changes in Y_{char} as a function of T and P . The contour plot shows that increasing the pyrolysis

temperature reduces charcoal yield, whereas increasing the pyrolysis pressure increases charcoal yield. The effect of the peak temperature corroborates the effect reported in earlier studies.^{12,18,40} In fact, when the temperature of pyrolysis increases, the chemical bonds in the biomass break down, leading to the formation of volatile substances, which, in turn, leads to a gradual reduction in the mass of the resulting char. The hydrogen and oxygen in the char are lost as the temperature increases, whereas the aromaticity and the carbonaceous nature of the char increase.⁴¹ The decrease in charcoal yield is partly due to gasification reactions at higher temperatures.⁴² In our study an increase in pressure was shown to lead to an increase in charcoal yield in agreement with results obtained in previous studies.^{18,20,21} The improvement in charcoal yield was due to the higher concentrations of pyrolytic volatile matter in the vapor phase inside the reactor, and not simply to an increase in the absolute pressure of the system. Rousset et al.¹⁸ reported that, in the case of eucalyptus wood subject to pyrolysis in a reactor with pressure of up to 10 bar, the positive effect of pressure was most pronounced between 0 and 5 bar. Conversely, during the pyrolysis of olive residues, Manyà et al.^{19,39,43} reported a decrease in charcoal yield with an increase in pyrolysis pressure. These authors concluded that the increase in charcoal yield could be explained by an increase in the vapor-phase residence time (and a corresponding decrease in both convective heat and mass transfer rates) in the packed bed, as well as by other factors, such as the nature of the biomass feedstock.³⁹

The results of the ANOVA for charcoal reactivity R are listed in Table 6. The model p -value (0.1643) of more than 0.05

Table 6. Analysis of Variance of the Average CO_2 Gasification Reactivity, $R(Y_2)$ ^a

source of variation	sum of squares	degrees of freedom	mean square	F-value	p-value prob > F
model	69.61	5	13.92	42.39	0.0001***
lack of fit	1.53	3	0.51	3.52	0.1643*

^aEffects: ***, most significant; *, nonsignificant at 5% probability.

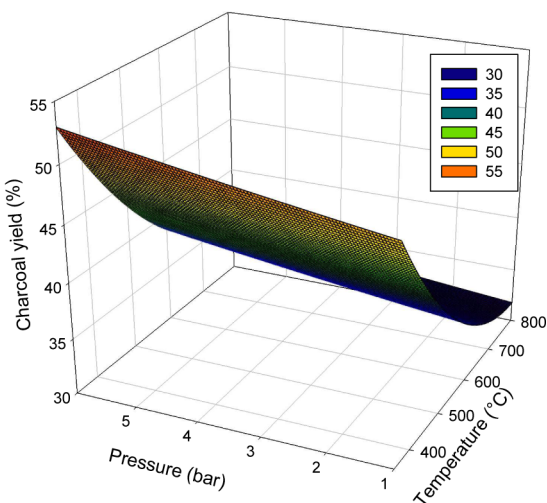
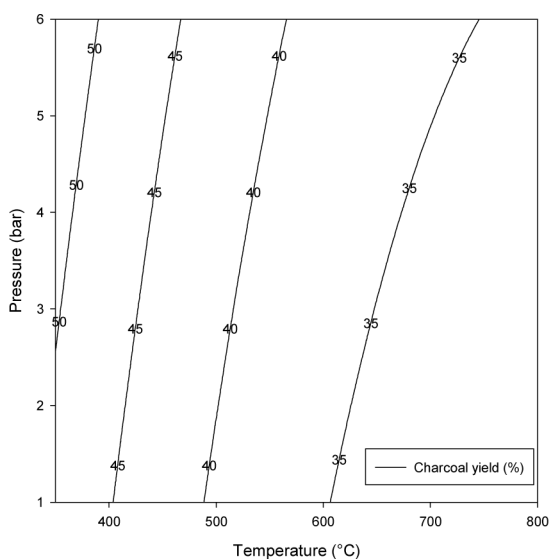


Figure 4. Contour plot showing the effects of peak temperature and absolute pressure on charcoal yield.

implies that the model results are not significant at a significance level of 5%. Since the results of the R^2 (0.949) and the p -value (more than 0.05) diverged, this could happen if there are more than the necessary number of regressors in the model with high collinearity among them. Another reason for the divergence between the p -value and R^2 is the size of the predictors. If the predictors are very small and if they are equally good at predicting the corresponding response, they will compete with each other for significance and the result may be a high p -value. We consequently had to analyze the average absolute deviation (AAD) to check the accuracy of the model.³⁸ The AAD is a direct method for describing deviations between the experimental and calculated responses.³⁷ The AAD is calculated by the following equation:

$$\text{AAD}/\% = \left\{ \left[\sum_{i=1}^p (|y_{i,\text{expt}} - y_{i,\text{calc}}|/y_{i,\text{expt}}) \right] / p \right\} \times 100 \quad (7)$$

where $y_{i,\text{expt}}$ and $y_{i,\text{calc}}$ are the experimental and calculated responses, respectively, and p is the number of experimental runs.

To check the accuracy of the model, it is preferable to evaluate the R^2 and AAD values together. R^2 must be close to 1.0, and AAD must be as small as possible. In our case, the calculated AAD value was 1.97%. These values and the resulting R^2 (0.949) show that the model equation satisfactorily describes the experimental design of R .

Table 7 lists the results of an ANOVA of the effect of the linear, interaction, and quadratic coefficients on charcoal

Table 7. Statistical Estimations of the Average CO_2 Gasification Reactivity, $R(Y_2)^a$

name	coefficient	F-inflation	std dev	F-value	p-value
β_1	-3.185	1.0	0.311198	418.95	0.0003***
β_2	-1.076	1.0	0.311198	47.88	0.0062**
β_{12}	0.172	1.0	0.381139	0.82	0.4321*
β_{11}	-0.566	1.125	0.466798	5.89	0.0937*
β_{22}	-0.331	1.125	0.466798	2.01	0.2509*

^aEffects: ***, most significant effect; **, less significant effect; *, effect not significant (probability level 5%).

reactivity. It can be seen that only the linear term of T and P is significant. The other coefficients (quadratic and interaction) have no significant effect (their corresponding p -value is more than 0.05). The nonsignificant interaction between the T and P term means that the influence of temperature does not depend on pyrolysis pressure. Moreover, T had a greater effect on charcoal reactivity than P (contribution term $\beta_1 = -3.185$ vs $\beta_2 = -1.076$). Figure 5 shows the two- and three-dimensional surface responses that were constructed to present the most important factors that influence reactivity. The contour plot of charcoal reactivity vs pressure and temperature (Figure 5) shows that increasing both peak temperature and absolute pressure during pyrolysis reduced charcoal reactivity.

Numerous studies in the literature discuss the effect of peak pyrolysis temperature and are in good agreement with our observations.^{44–47} Although high pyrolysis temperatures created chars with many small pores, thinner cell walls, and larger surface area, char gasification reactivity decreased due to the difficulties CO_2 had accessing the micropore structure of the char. Yuan et al.⁴⁵ confirmed this observation by showing that the decrease in gasification reactivity with increasing

pyrolysis temperature was due to an increase in uniformity and in the degree of graphitization of the resulting char. Fermoso et al.⁴⁶ reported that the decrease in gasification reactivity may also be due to the ordering of the carbon matrix and a reduction in the concentration of active sites.

Concerning the effect of pressure, previous works provided evidence that increasing pressure during pyrolysis reduces the CO_2 gasification reactivity of the resulting charcoal.^{22,48,49} Despite the fact these studies were conducted under more severe pyrolysis conditions (higher heating rate, high temperature, and high pressure) than the ones we applied in our experiments, we observed the same effect of pyrolysis pressure on CO_2 gasification reactivity of the resulting charcoal. According to Okumura et al.,²² the decrease in CO_2 gasification reactivity of the charcoal with pyrolysis pressure is due to the increased uniformity of the carbonaceous structure of charcoal with increasing pyrolysis pressure. Cetin et al.⁴⁷ found that char produced at 20 bar reacts approximately three times more slowly than char generated at atmospheric pressure. Pyrolysis pressure influenced the size and the shape of particles, and we observed a general increase in the proportion of voids and a decrease in the thickness of the cell walls of charcoal particles with an increase in pyrolysis pressure. We thus obtained charcoal with a small surface area and an increase graphitization or a lower oxygen content, which reduced the reactivity of the resulting charcoal.

3.2. Optimizing the Preparation of Reductant Charcoal. The aim of this study was to identify optimal conditions for the preparation of charcoal with good characteristics to be used in blast furnaces. For the correct functioning of a blast furnace, the reductant must have high fixed carbon and low CO_2 gasification reactivity. To achieve this, pyrolysis must be conducted at high temperatures, which reduces charcoal yield, involves costly pyrolysis operations, and makes it difficult to obtain homogeneous charcoal (due to the difficulty involved in maintaining a uniform temperature in the reactor). To reduce costly and operating risks and to increase the yield of charcoal, the temperature of pyrolysis needs to be reduced. Because of its positive effect on charcoal properties (i.e., an increase in charcoal yield and a decrease in charcoal reactivity), pyrolysis under pressure is recommended coupled with low pyrolysis temperature. The comparison of optimal conditions for responses Y_1 and Y_2 revealed that the maximization of each response was not possible in the same conditions. To determine an acceptable compromise, responses were simultaneously optimized by using the desirability functions approach, which is included in the Statgraphics software

This method first converts each estimated response Y_i into an individual scale-free desirability function d_i that varies over the range of 0 outside the desired limits (if $Y_i(x) \leq Y_{i,\text{min}}$) to 1 the target (desired) value (if $Y_i(x) \geq Y_{i,\text{max}}$) where $Y_{i,\text{min}}$ and $Y_{i,\text{max}}$ are the lower and upper bounds of acceptability for response i , respectively. The lower and upper acceptability bounds were set at the extreme values, selected according to the desired quality of the reductant charcoal, and of the individual estimated response, since the response surface had been reasonably explored in the range of variables studied here. The weights of the response variables were all set to one, because all responses were considered to be equally important

Once the function d_i has been defined for each response of interest, an overall objective function (D), representing the overall desirability function, is calculated by determining the geometric mean of the individual desirabilities. Hence, the

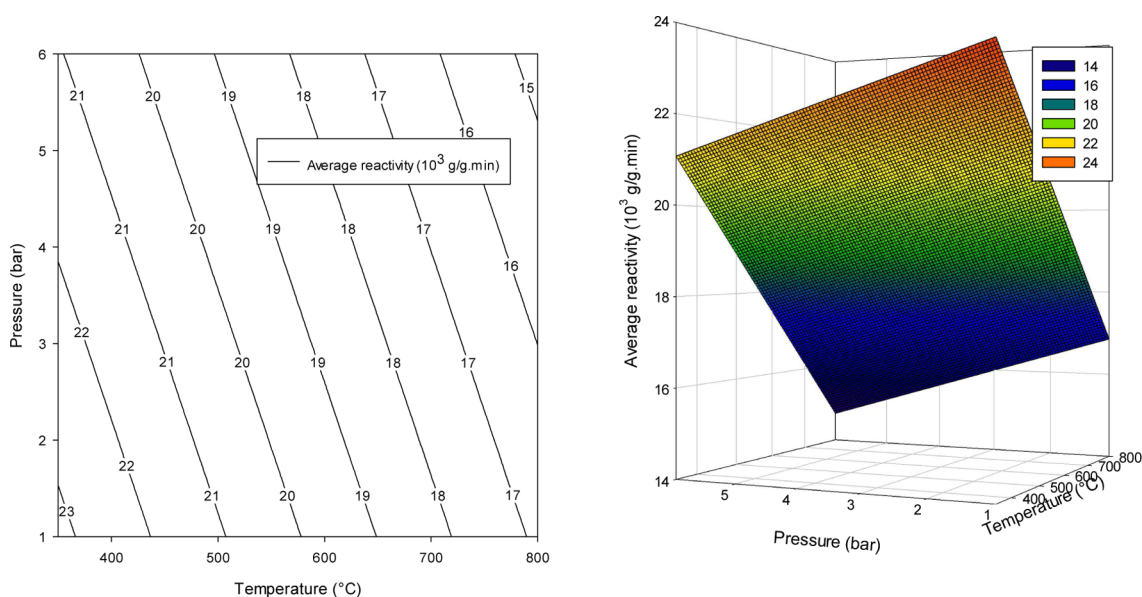


Figure 5. Contour plot showing the effects of peak temperature and absolute pressure on CO₂ gasification reactivity of acacia charcoal during pyrolysis.

function D over the experimental domain is calculated using eq 8 as follows:⁵⁰

$$D = (d_1(Y_1) d_2(Y_2))^{1/2} \quad (8)$$

For optimization, each response function has reduced to the contribution of only the significant terms based on the results of the ANOVA (i.e., β_1 , β_2 , and β_{11} for charcoal yield and β_1 and β_2 for charcoal CO₂ reactivity). The optimum condition for preparation of reductant charcoal from acacia wood in the pressurized macro-TG was found to be a peak temperature of 617 °C and 6 bar of absolute pressure. Under these conditions, the charcoal yield and the average CO₂ gasification reactivity of charcoal would be 38% and 16.965×10^{-3} g/(g·min), respectively. These optimal pyrolysis conditions are in the same order of magnitude as those found by Rousset et al. (optimal temperature of 600 °C and pressure of 10 bar).¹⁸

4. CONCLUSIONS

In the present work, the effect of both the absolute pressure (range 1–6 bar) and peak temperature (range 350–800 °C) during pyrolysis of *Acacia senegal* wood in a macro-TG on the yield and CO₂ gasification reactivity of the obtained charcoal were analyzed. ANOVA was used to identify the significant factors. Below is an itemized list of our findings and major conclusions.

- (1) The experimental responses (charcoal yield and charcoal CO₂ gasification reactivity) satisfactorily agreed with model predictions.
- (2) An increase in pyrolysis pressure led to an increase in charcoal yield.
- (3) An increase in both the absolute pressure and peak temperature during pyrolysis led to a decrease in the CO₂ gasification reactivity of the resulting charcoal.
- (4) The interaction between temperature and pressure had no significant influence on charcoal reactivity.
- (5) Peak temperature had a more significant impact on the CO₂ gasification reactivity of the resulting charcoal than absolute pressure.

- (6) The optimum conditions for the preparation of reductant charcoal were found to be a peak pyrolysis temperature of 617 °C and an absolute pressure of 6 bar.

AUTHOR INFORMATION

Corresponding Author

*E-mail: joel.blin@ciraf.fr.

Present Address

[†]Joint Graduate School of Energy and Environment, Centre of Excellence on Energy Technology and Environment, King Mongkut's University of Technology Thonburi, Bangkok Thailand.

Funding

The authors gratefully acknowledge the financial support of AIRD/Cirad.

Notes

The authors declare no competing financial interest.

ABBREVIATIONS

- AAD = the absolute average deviation
- D = overall objective function
- db = dry basis
- FCCCD = face-centered central composite design
- m = instantaneous sample mass during the gasification stage (g)
- m_{ash} = charcoal ash content (g)
- m_b = dry mass of acacia sample (g)
- m_{char} = mass of resulting charcoal (g)
- m_0 = initial mass of sample at the beginning of gasification stage (g)
- m_1 = charcoal mass at time t_1 during the gasification stage (g)
- m_2 = charcoal mass at time t_2 during the gasification stage (g)
- P = absolute pressure
- R = charcoal CO₂ gasification reactivity at time t (g/(g·min))
- R^2 = coefficient of determination
- R^2_{adj} = adjusted coefficient of determination
- RSM = response surface methodology
- T = peak temperature

t = time (min)
 t_1 = time at the start of the weight measurements during the gasification stage (min)
 t_2 = time at the end of the weight measurement during the gasification stage (min)
 X = degree of conversion of charcoal during the gasification stage (%)
 X_1 = coded variable for temperature
 X_2 = coded variable for pressure
 Y_{char} = charcoal yield (%)

Greek Symbols

β_0 = regression coefficient for the intercept term
 β_1 = regression coefficient for the linear effect of temperature
 β_2 = regression coefficient for the linear effect of pressure
 β_{11} = regression coefficient for the quadratic effect of temperature
 β_{12} = regression coefficient for the interaction term
 β_{22} = regression coefficient for the quadratic effect of pressure

REFERENCES

- (1) Yoshida, T.; Turn, S. Q.; Yost, R. S.; Antal, M. J. *Ind. Eng. Chem. Res.* **2008**, *47*, 9882–9888.
- (2) Norgate, T.; Haque, N.; Somerville, M.; Jahanshahi, S. *ISIJ Int.* **2012**, *52*, 1472–1481.
- (3) Norgate, T.; Langberg, D. *ISIJ Int.* **2009**, *49*, 587–595.
- (4) Söderman, J.; Saxén, H.; Pettersson, F. *Comput.-Aided Chem. Eng.* **2009**, *26*, 567–571.
- (5) Mathieson, J. G.; Rogers, H.; Somerville, M.; Jahanshahi, S.; Ridgeway, P. In *Chemeca 2011: Engineering a Better World*.
- (6) Griessacher, T.; Antrekowitsch, J.; Steinlechner, S. *Biomass Bioenergy* **2012**, *39*, 139–146.
- (7) Agirre, I.; Griessacher, T.; Rösler, G.; Antrekowitsch, J. *Fuel Process. Technol.* **2013**, *106*, 114–121.
- (8) Suopajarvi, H.; Pongrácz, E.; Fabritius, T. *Renewable Sustainable Energy Rev.* **2013**, *25*, 511–528.
- (9) Suopajarvi, H.; Fabritius, T. *Sustainability* **2013**, *5*, 1188–1207.
- (10) Fick, G.; Mirgaux, O.; Neau, P.; Patisson, F. *Carbon Management Technology Conference*, Alexandria, VA, USA, Oct. 21–23, 2013; Founder Societies: Technologies for Carbon Management, 2013.
- (11) Fick, G.; Mirgaux, O.; Neau, P.; Patisson, F. *Waste Biomass Valorization* **2014**, *5*, 43–55.
- (12) Antal, M. J.; Grønli, M. *Ind. Eng. Chem. Res.* **2003**, *42*, 1619–1640.
- (13) Balat, M. *Energy Sources, Part A* **2008**, *30*, 636–648.
- (14) Gupta, R. C. *Miner. Process. Extr. Metall. Rev.* **2003**, *24*, 203–231.
- (15) Diez, M. A.; Alvarez, R.; Barriocanal, C. *Int. J. Coal Geol.* **2002**, *50*, 389–412.
- (16) Pereira, B. L. C.; Oliveira, A. C.; Carvalho, A. M. M. L.; Carneiro, A. d. C. O.; Santos, L. C.; Vital, B. R. *Int. J. For. Res.* **2012**, *2012*, 523025.
- (17) Kumar, M.; Gupta, R. C.; Sharma, T. *Fuel Process. Technol.* **1992**, *32*, 69–76.
- (18) Rousset, P.; Figueiredo, C.; De Souza, M.; Quirino, W. *Fuel Process. Technol.* **2011**, *92*, 1890–1897.
- (19) Manyà, J. J.; Roca, F. X.; Perales, J. F. *J. Anal. Appl. Pyrolysis* **2013**, *103*, 86–95.
- (20) Antal, M. J., Jr.; Croiset, E.; Dai, X.; DeAlmeida, C.; Mok, W. S.-L.; Norberg, N.; Richard, J.-R.; Al Majthoub, M. *Energy Fuels* **1996**, *10*, 652–658.
- (21) Antal, M. J., Jr.; Allen, S. G.; Dai, X.; Shimizu, B.; Tam, M. S.; Grønli, M. *Ind. Eng. Chem. Res.* **2000**, *39*, 4024–4031.
- (22) Okumura, Y.; Hanaoka, T.; Sakanishi, K. *Proc. Combust. Inst.* **2009**, *32*, 2013–2020.
- (23) Kumar, M.; Verma, B. B.; Gupta, R. C. *Energy Sources* **1999**, *21*, 675–685.
- (24) Khider, T. O.; Elsaki, O. T. *J. For. Prod. Ind.* **2012**, *1*, 5–9.
- (25) Meincken, M.; Tyhoda, L. *Biomass Quality*. In *Bioenergy from Wood*; Seifert, T., Ed.; Managing Forest Ecosystems; Springer: Dordrecht, The Netherlands, 2014; Vol. 26, p 169, DOI: [10.1007/978-94-007-7448-3_8](https://doi.org/10.1007/978-94-007-7448-3_8).
- (26) Petroff, G.; Doat, J. *Bois For. Trop.* **1978**, *51*–64.
- (27) Daouk, E.; Van de Steene, L.; Paviet, F.; Salvador, S. *Chem. Eng. Sci.* **2015**, *126*, 608–615.
- (28) Kumar, M.; Gupta, R. C. *Fuel Process. Technol.* **1994**, *38*, 223–233.
- (29) Chen, G.; Yu, Q.; Sjöström, K. *J. Anal. Appl. Pyrolysis* **1997**, *40*–41, 491–499.
- (30) Moilanen, A. *Thermogravimetric characterisations of biomass and waste for gasification processes*; VTT Publications: Espoo, Finland, 2006.
- (31) Degroot, W. F.; Shafizadeh, F. *Fuel* **1984**, *63*, 210–216.
- (32) Barrio, M.; Göbel, B.; Rimes, H.; Henriksen, U.; Hustad, J. E.; Sørensen, L. H. *Steam Gasification of Wood Char and the Effect of Hydrogen Inhibition on the Chemical Kinetics*. In *Progress in Thermochemical Biomass Conversion*; Bridgwater, A. V., Ed.; Blackwell Science: Oxford, U.K., 2001; Vol. 1, pp 32–46.
- (33) Ollero, P.; Serrera, A.; Arjona, R.; Alcantarilla, S. *Biomass Bioenergy* **2003**, *24*, 151–161.
- (34) Zhang, Y.; Ashizawa, M.; Kajitani, S.; Miura, K. *Fuel* **2008**, *87*, 475–481.
- (35) Gomez-Barea, A.; Ollero, P.; Arjona, R. *Fuel* **2005**, *84*, 1695–1704.
- (36) Huo, W.; Zhou, Z.; Chen, X.; Dai, Z.; Yu, G. *Bioresour. Technol.* **2014**, *159*, 143–149.
- (37) Baş, D.; Boyacı, İ. H. *J. Food Eng.* **2007**, *78*, 836–845.
- (38) Harris, L. N. *Qual. Reliab. Eng. Int.* **1987**, *3*, 212.
- (39) Manyà, J. J.; Laguarda, S.; Ortigosa, M. A.; Manso, J. A. *Energy Fuels* **2014**, *28*, 3271–3280.
- (40) Sharma, A.; Pareek, V.; Wang, S.; Zhang, Z.; Yang, H.; Zhang, D. *Comput. Chem. Eng.* **2014**, *60*, 231–241.
- (41) Sharma, R. K.; Hajaligol, M. R.; Martoglio Smith, P. A.; Wooten, J. B.; Baliga, V. *Energy Fuels* **2000**, *14*, 1083–1093.
- (42) Encinar, J. M.; González, J. F.; González, J. *Fuel Process. Technol.* **2000**, *68*, 209–222.
- (43) Manyà, J. J.; Ortigosa, M. A.; Laguarda, S.; Manso, J. A. *Fuel* **2014**, *133*, 163–172.
- (44) Min, F.; Zhang, M.; Zhang, Y.; Cao, Y.; Pan, W. *J. Anal. Appl. Pyrolysis* **2011**, *92*, 250–257.
- (45) Yuan, S.; Chen, X.; Li, J.; Wang, F. *Energy Fuels* **2011**, *25*, 2314–2321.
- (46) Feroso, J.; Stevanov, C.; Moghtaderi, B.; Arias, B.; Pevida, C.; Plaza, M. G.; Rubiera, F.; Pis, J. J. *J. Anal. Appl. Pyrolysis* **2009**, *85*, 287–293.
- (47) Cetin, E.; Moghtaderi, B.; Gupta, R. C.; Wall, T. F. *Fuel* **2004**, *83*, 2139–2150.
- (48) Melligan, F.; Auccaise, R.; Novotny, E. H.; Leahy, J. J.; Hayes, M. H. B.; Kwapinski, W. *Bioresour. Technol.* **2011**, *102*, 3466–3470.
- (49) Newalkar, G.; Iisa, K.; D'Amico, A. D.; Sievers, C.; Agrawal, P. *Energy Fuels* **2014**, *28*, 5144–5157.
- (50) Ennaciri, K.; Baçaoui, A.; Sergent, M.; Yaacoubi, A. *Chemom. Intell. Lab. Syst.* **2014**, *139*, 48–57.

NOTE ADDED AFTER ASAP PUBLICATION

This paper was published on the Web on October 29, 2015, with minor text errors in section 2.2. The corrected version was reposted on November 3, 2015.